

POLARIZATION OF STARLIGHT BY AN UNRESOLVED AND OBLATE EXTRASOLAR PLANET IN AN ELLIPTICAL ORBIT

SUJAN SENGUPTA AND MALAY MAITI

Indian Institute of Astrophysics, Koramangala, Bangalore 560 034, India; sujan@iiap.res.in, mith@iiap.res.in

Received 2005 July 11; accepted 2005 November 7

ABSTRACT

We calculate the degree of linear polarization of radiation from stars having planets that may not be spatially resolved. We assume single scattering by water and silicate particulates in the planetary atmosphere. The dilution of the reflected polarized radiation of the planet by the unpolarized stellar radiation and the effect of the oblateness of the planet, as well as its elliptical orbit, are included. We employ a chemical equilibrium model to estimate the number density of water and silicate condensates and calculate the degree of linear polarization at the R band of starlight as a function of (1) mean size of condensates, (2) planetary oblateness, (3) inclination angle, (4) phase angle, (5) orbital eccentricity e , and (6) epoch of periastron passage. We show that the polarization profile alters significantly at all inclination angles when an elliptical orbit is considered, and the degree of polarization peaks at the epoch of periastron passage. We predict that a detectable amount of linear polarization may arise if the planetary atmosphere is optically thin, the mean size of the condensates is not greater than a few microns, and the oblateness of the planet is as high as that of Jupiter.

Subject headings: binaries: general — dust, extinction — planetary systems — polarization — scattering

1. INTRODUCTION

Polarization has always been an efficient tool to probe the physical properties in the environment of various astrophysical objects. Recently, it has been realized that polarization could be a very important diagnostic method for analyzing the atmosphere of substellar massive objects such as brown dwarfs and extrasolar planets. Sengupta & Krishan (2001) predicted a detectable amount of linear polarization from L dwarfs because of the presence of condensates in the visible atmosphere; subsequently, linear polarization in the optical bands was detected by Menard et al. (2002) and Zapatero Osorio et al. (2005). The observed linear polarization can be explained well by single dust scattering models that assume an optically thin and rotationally oblate photosphere (Sengupta 2003; Sengupta & Kwok 2005).

On the other hand, the use of polarimetry in detecting and understanding the physical properties of extrasolar planets is emphasized by Seager et al. (2000), Saar & Seager (2003), and Stam et al. (2004). While Seager et al. (2000) modeled the polarization due to close-in planets or so-called roasters, such as the first-discovered extrasolar planet, 51 Peg b (Mayor & Queloz 1995), Stam et al. (2004) estimated the degree of polarization caused by a planet at Jupiter's distance from the Sun. In both methods, the reflected flux of the planet and the Stokes vectors of the reflected radiation are calculated by assuming a circular orbit and blackbody radiation from the star. The planet is considered to be spherical and the polarization is integrated over the illuminated portion of the disk. While multiple scattering polarization was calculated by Stam et al. (2004), Seager et al. (2000) employed a Monte Carlo procedure and computed the number of scatterings. The latter authors found that for an almost absorbing atmosphere, a higher amount of polarization may arise due to single scattering. In both investigations, the observable degree of polarization is estimated by simply multiplying the flux ratio by the polarization of the radiation from the spatially resolved planet. Since degree of polarization is a relative measure, it does not carry any information about the radius of the circular orbit or the planetary radius.

However, in the most realistic situation, the planet should be oblate because of rotation around its own axis. The oblateness of

solar planets ranges from 0.003 for Earth to 0.065 for Jupiter and 0.1 for Saturn. Furthermore, most of the extrasolar planets detected so far have eccentric orbits around their stars, with the eccentricity ranging from 0.0 to as high as 0.7.

Although multiple scattering is a reasonable choice for an optically thick medium, it underestimates the amount of polarization by a few orders of magnitude if the medium is optically thin and hence polarization is caused by single scattering. As mentioned before, single scattering polarization could successfully explain the high degree of linear polarization observed from L dwarfs. Therefore, it is quite reasonable to investigate the amount of polarization that could arise due to single scattering in extrasolar planets.

In this paper, we present polarization profiles of starlight caused by single scattering in the atmosphere of an oblate planet rotating in elliptical orbit and show that in certain cases the polarization may be detectable by existing instrumental facilities.

2. SINGLE SCATTERING POLARIZATION OF STARLIGHT

Since the dust density is assumed to be low and scattering by atoms and molecules (e.g., Rayleigh scattering) does not contribute significantly to polarization, a single-scattering approximation is reasonable for a region where the optical depth $\tau < 1$. If present, multiple scattering can reduce the degree of polarization by a few orders of magnitude (Sengupta & Krishan 2001) because the planes of the scattering events are randomly oriented and average out each other's contribution to the final polarization. Hence, the amount of observed linear polarization could act as a probe to decide in favor of a single- or multiple-scattering approximation.

In the present work, we use the formalism given by Simmons (1983), which is a generalization of the work by Brown et al. (1978). In this formalism, the primary star is assumed to be a point source of unpolarized light. For most practical applications, the Stokes parameters are normalized and defined by $(I_{\text{refl}}, Q, U, V)/I_{\text{total}}$, where $I_{\text{total}} = I_{\text{refl}} + I_{\text{star}}$, I_{refl} is the reflected flux or intensity from the planet, and I_{star} is the unpolarized flux or intensity received from the star. We have neglected the thermal radiation

of the planet, if any, because for a sufficiently old planet the thermal radiation should be much less than the reflected radiation, or there may not be thermal radiation by comparatively smaller, earthlike planets. However, for young giant planets far away from the primary star, thermal radiation should be significant. Since I_{refl} is much less than I_{star} , we consider $I_{\text{total}} = I_{\text{star}}$, and hereafter treat I_{refl} , Q , U , and V as normalized Stokes parameters. Hence, the degree of linear polarization can be written as $P = (Q^2 + U^2)^{1/2}$.

The density distribution of the scatterer is calculated in a corotating reference frame, so that it is independent of the phase angle Λ of the planet. The transformation to the observer frame is made by using the properties of spherical harmonics under rotation. In a circular orbit, the normalized Stokes parameters Q and U are given as a harmonic series:

$$Q(k, i, \Lambda) = \sum_{m=0}^{\infty} [p_m(k, i) \cos m\Lambda + q_m(k, i) \sin m\Lambda], \quad (1)$$

$$U(k, i, \Lambda) = \sum_{m=0}^{\infty} [u_m(k, i) \cos m\Lambda + v_m(k, i) \sin m\Lambda], \quad (2)$$

where $k = 2\pi/\lambda$, λ is the wavelength and i is the orbital inclination angle. The harmonic coefficients are given by

$$\begin{pmatrix} p_m \\ q_m \end{pmatrix} = \frac{2\pi}{k^2} \sum_{l=M}^{\infty} F_{l2}(k) G_m^l(i) \begin{pmatrix} \eta_{lm} \\ \xi_{lm} \end{pmatrix}, \\ m = 0, 1, 2, 3, \dots, \quad (3)$$

$$\begin{pmatrix} u_m \\ v_m \end{pmatrix} = \frac{2\pi}{k^2} \sum_{l=M}^{\infty} F_{l2}(k) H_m^l(i) \begin{pmatrix} -\xi_{lm} \\ \eta_{lm} \end{pmatrix}, \\ m = 0, 1, 2, 3, \dots, \quad (4)$$

where $M = \max(2, m)$, and $G_m^l(i)$ and $H_m^l(i)$ are given in Simmons (1983). In addition, η_{lm} and ξ_{lm} are related to the density distribution in the corotating frame and are given by

$$\begin{pmatrix} \eta_{lm} \\ \xi_{lm} \end{pmatrix} = \alpha(l, m) \\ \times \int n'(r, \theta, \phi) P_l^m(\cos \theta_i) \begin{pmatrix} \cos m\phi \\ \sin m\phi \end{pmatrix} \sin \theta d\theta d\phi dr, \quad (5)$$

where $n'(r, \theta, \phi)$ is the number density of the scatterer in the corotating frame, θ_i is the viewing angle, P_l^m is the associated Legendre function of the first kind, and

$$\alpha(l, m) = \left[\frac{(2l+1)(l-m)}{4\pi(l+m)} \right]^{1/2}. \quad (6)$$

At an edge-on view, $\theta_i = \pi/2$ and $\phi = 0$, and hence $\xi_{lm} = 0$. The term $F_{l2}(k)$ is related to the scattering function and is given by

$$F_{lm} = \alpha(l, m) \int_{-1}^1 \frac{i_1(k, \theta) - i_2(k, \theta)}{2} P_l^m(\cos \theta) d(\cos \theta). \quad (7)$$

In the above equation, θ is the scattering angle and i_1 and i_2 are the scattering functions given by van de Hulst (1957), which depend on the refractive index as well as on the size and shape of the scatterer. In the present work we consider spherical dust particles as the scatterer.

Considering an ellipsoidal density distribution and using the addition theorem of spherical harmonic, η_{lm} can be written as

$$\eta_{lm} = 2\pi\alpha(l, m) P_l^m(0) \int_{R_2}^{R_1} n(r) dr \int_{-1}^1 \frac{P_l(\mu) d\mu}{[1 + (A^2 - 1)\mu^2]^{1/2}}, \quad (8)$$

where R_1 and R_2 are the outer and inner equatorial axis length of the planet, A is the ratio of the length of the equatorial axis to the polar axis, and $\mu = \cos \theta$. We have taken multipoles up to $l = 5$. We have considered up to the fifth harmonic, i.e., $m = 0, 1, 2, 3, 4, 5$. However, since the density distribution is symmetric about the orbital plane, the first, third, and fifth harmonics are zero, and the fourth harmonic is small compared to the second harmonic. In other words, for the adopted density distribution, the odd-numbered harmonics are zero, and the degree of polarization is determined mainly by the second harmonic.

We convert $n(r)dr$ into $n(P)dP$ by using the equation of hydrostatic equilibrium $n(r)dr = n(P)dP/g\rho(P)$, where P is the pressure at different geometrical heights, ρ is the mass density at different pressure scales, and g is the surface gravity (which can be assumed to be constant for a geometrically thin atmosphere). The degree of polarization is calculated at wavelengths ranging from 0.5486 to 0.8491 μm and averaged by using the response function of the R -band Bessel filter.

3. EFFECT OF ORBITAL ECCENTRICITY

The effect of orbital eccentricity enters through a multiplicative factor $h(\Lambda, e)$ to the coefficient of the dominant harmonic p_2 and v_2 (Brown et al. 1982) and is given by

$$h(\Lambda, e) = \frac{[1 + e \cos(\lambda - \lambda_p)]^2}{(1 - e^2)^2}, \quad (9)$$

where e is the orbital eccentricity and λ is the true anomaly, which is related to the eccentric anomaly E by

$$\tan\left(\frac{\lambda - \lambda_p}{2}\right) = \left(\frac{1+e}{1-e}\right)^{1/2} \tan\frac{E}{2}, \quad (10)$$

where λ_p is the longitude of the periastron. The eccentric anomaly E is related to the orbital phase angle through Kepler's equation,

$$E - e \sin E = \Lambda - \Lambda_p, \quad (11)$$

where $\Lambda - \Lambda_p = 2\pi(t - T_0)/P$ is the mean anomaly, t is any epoch of time, P is the orbital period, and T_0 is the epoch of periastron passage. We have assumed that there is no drastic seasonal change in the planetary atmosphere and that the atmospheric temperature-pressure (T-P) profile remains the same throughout the planetary year.

For a circular orbit, the polarization profile is determined by the second harmonic only. But for an elliptical orbit, the first and third harmonics are nonzero, although the second harmonic remains dominant.

4. THE ATMOSPHERIC MODELS

We have adopted the atmospheric models of extrasolar planets given in Sudarsky et al. (2003). The T-P profiles are taken for models of class II and V planets or close-in planets, also known as roasters. The atmospheres of class II planets should have water as a condensate, while class V planets should contain silicate in their

upper atmospheres. In calculating the T-P profile of the planet *v* And d (a class II planet), Sudarsky et al. (2003) considered the surface gravity to be $2 \times 10^4 \text{ cm s}^{-2}$, while for the planet HD 209458b (a class V planet) the surface gravity is taken to be 980 cm s^{-2} . In the present work, we have taken the same values for the surface gravity of the two representative planets. We have assumed that the thermal radiation of the planet is negligible compared to the reflected radiation, so that the contribution to polarization comes only from the reflected radiation.

The dust distribution in the atmosphere is calculated based on the one-dimensional cloud model of Cooper et al. (2003). This model assumes chemical equilibrium throughout the atmosphere, and a uniform density distribution across the surface of an object at each given pressure and temperature. Under these assumptions, the number density of cloud particles is given by

$$n(P) = q_c \left(\frac{\rho}{\rho_d} \right) \left(\frac{\mu_d}{\mu} \right) \left(\frac{3}{4\pi r^3} \right), \quad (12)$$

where ρ is the mass density of the surrounding gas, r is the cloud particle radius, ρ_d is the mass density of the dust condensates, and μ and μ_d are the mean molecular weight of atmospheric gas and condensates, respectively. The condensate mixing number ratio (q_c) is given as $q_c = q_{\text{below}} P_{c,l}/P$ for heterogeneously condensing clouds, where q_{below} is the fraction of condensable vapor just below the cloud base, $P_{c,l}$ is the pressure at the condensation point, and P is the gas pressure in the atmosphere. The condensation curves for water and forsterite condensates are taken from Sudarsky et al. (2003). The values of μ_d , ρ_d and q_{below} for forsterite and water are taken from Cooper et al. (2003). The real part of the refractive index for forsterite is fixed at 1.65 at any wavelength and the imaginary part is taken by interpolating the data given in Scott & Duley (1996). For the refractive index of water, we have used the data given in Segelstein (1981).

Apart from the calculation of the grain number density, the location of the cloud in the atmosphere plays an important role in determining the amount of polarization. The location of the cloud base for different atmospheric models and different chemical species is determined by the intersection of the T-P profile of the atmosphere model and the condensation curve $P_{c,l}$ as prescribed in Cooper et al. (2003). Taking the condensation curve for forsterite and water as given in Sudarsky et al. (2003), we determine the base of the cloud from the T-P profiles of *v* And d and HD 209458 b as calculated by the same authors.

At present, there is no convincing justification in favor of any specific form of the particle size distribution function. In the present work, we adopt a lognormal size distribution function used by Ackerman & Marley (2001) and Saumon et al. (2000) with a width fixed at 1.3. Following Sudarsky et al. (2003), we have taken the mean particle radius for water as $5.0 \mu\text{m}$ and that for silicate (forsterite) as $10.0 \mu\text{m}$. However, in order to show the effect of mean grain size on the degree of polarization, we have also presented the polarization profile as a function of mean particle size, keeping the T-P profile the same as that calculated by Sudarsky et al. (2003) for water, with mean grain size $5.0 \mu\text{m}$.

In multiple scattering, the mean particle size should be different at different pressure scales. However, for single scattering, a fixed mean particle size of a particular condensate is sufficient (Sengupta & Kwok 2005).

5. THE OBLATENESS OF PLANETS

The rotationally induced oblateness of solar planets has been discussed in detail by Hubbard (1984) and Murray & Dermott

(2000). Recently, the formalism for oblateness has been extended to extrasolar planets by Barnes & Fortney (2003), who used the Darwin-Radau relationship (Murray & Dermott 2000; Barnes & Fortney 2003)

$$f = \frac{\Omega^2 R_e^3}{GM} \left[\frac{5}{2} \left(1 - \frac{3}{2} K \right)^2 + \frac{2}{5} \right]^{-1} \quad (13)$$

to relate rotation to oblateness. In the above equation, $K = I/MR_e^2 \leq 2/3$ is the moment-of-inertia parameter of an object with moment of inertia I . The Darwin-Radau relationship is exact for uniform-density objects ($K = 0.4$) and provides a reasonable (within a few percent error) estimation of the oblateness of the solar planets. At a 1 bar pressure level, the oblateness f of Jupiter, Saturn, and Earth are 0.065, 0.098, and 0.003, respectively. Barnes & Fortney (2003) modeled the planet HD 209458b and estimated its oblateness to be about 0.00285. Apart from rotational effects, the tidal interaction of a close-in planet with its primary star may also impose an ellipsoidal shape extending toward the star. In the present work we ignore such effects. Moreover, the estimation of the moment of inertia of a planet needs the density distribution, radius, and mass of the planet along with its rotational period, and so is highly model dependent. In the present work we adopt a wide range of values for oblateness; the maximum value is equal to that of Jupiter ($f = 0.065$), and the minimum value is equal to that of Earth ($f = 0.003$).

6. RESULTS AND DISCUSSION

We present in Figures 1 and 2 the polarization profiles at the *R* band (Bessel filter) of a star with a planet having forsterite as a major condensate in its atmosphere. Silicate and iron can form high in the atmosphere of class V roasters that orbit their stars around 0.05 AU. Although the presence of more than one species affects the amount of polarization because of differences in size, optical properties, and location, we assume forsterite to be the major condensate in our model, for simplicity. However, the change in the amount of polarization by the incorporation of other condensate species cannot be determined due to the dominant effect of other parameters, such as inclination angle, orbital eccentricity, oblateness, etc. Figure 3 presents the degree of polarization as a function of planetary oblateness. Figure 4 presents the polarization profile for planets with noncircular orbits, and the change in degree of polarization caused by the change in orbital eccentricity is shown in Figure 5.

Our polarization profiles for the orbital eccentricity $e = 0$, i.e., for circular orbits, presented in Figures 1 and 2, are qualitatively the same as that presented by Stam et al. (2004). When the inclination angle $i = 0$, the observed part of the planet that is illuminated is constant, and hence the degree of polarization is constant. The maximum amount of polarization produced by the planet is the same for all values of i . When the inclination angle $i = 90^\circ$, the polarization is zero at the fractional orbital period $t/P = 0.25$ and 0.75 , corresponding to the phase angles $\Lambda = 180^\circ$ and 0° , respectively, because the planet's night and day sides are turned toward the observer in these cases. Apart from the geometrical asymmetry of any object, another asymmetry plays an important role in determining the polarization profile for a binary star or a planet orbiting around a star. This second effect is due to the asymmetry in the position of the object (or the scatterer) with respect to the observer and the source of light. As the symmetry axis of the planet changes position with respect to the observer, the total number of effective scatterers also changes. This effect can be visualized as the amount of light that

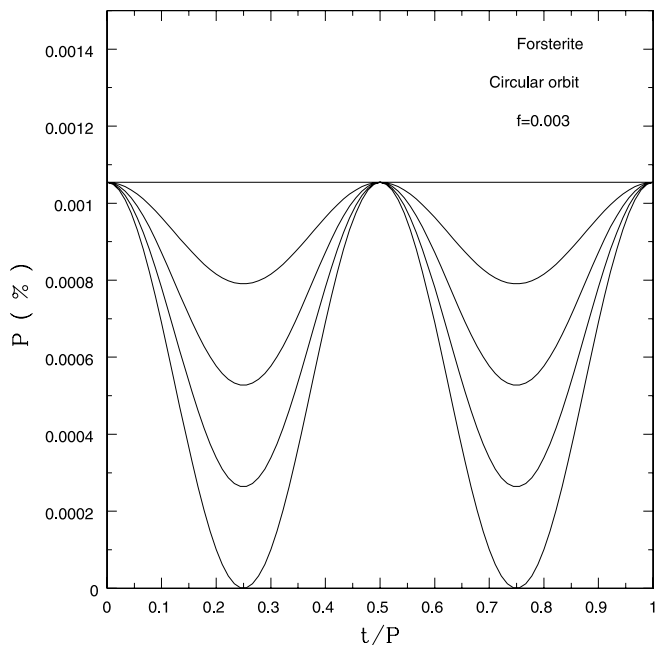


FIG. 1.—Degree of linear polarization at Bessel *R* band caused by forsterite grain with mean radius $r_0 = 10 \mu\text{m}$. The polarization is plotted as a function of the fractional orbital period t/P , where t is time and P is the orbital period. Models are for a planet with oblateness $f = 0.003$ and a circular orbit. From bottom to top, the curves represent polarization with inclination angles $i = 90^\circ, 60^\circ, 45^\circ, 30^\circ$ and 0° , respectively.

is scattered toward the observer from the net illuminated region. In a circular orbit, the observed degree of polarization is determined by the scatterers that are present within the illuminated area facing toward the observer. The observed degree of polarization is zero when the night side of the object is toward the observer, and it increases as the illuminated area toward the observer increases. The fraction of the area that is illuminated depends on the inclination angle as well. As the inclination angle decreases, the orbital plane becomes more and more face-on toward the observer.

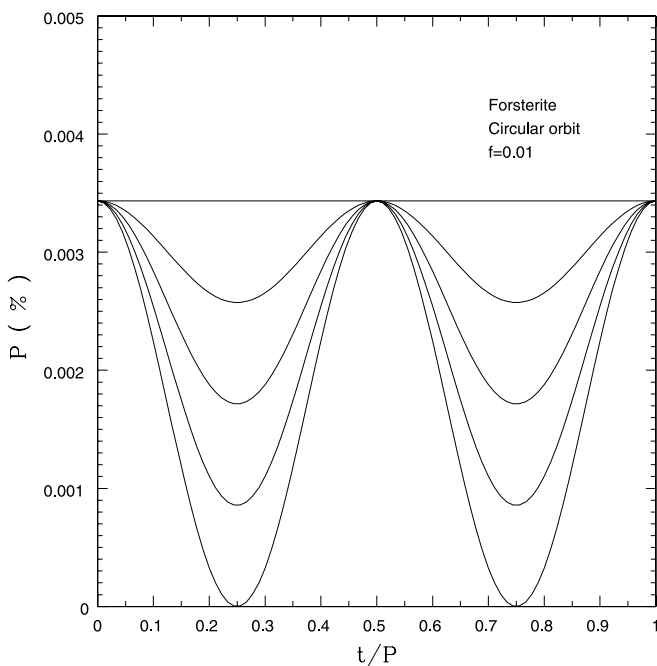


FIG. 2.—Same as Fig. 1, but for a planet with oblateness $f = 0.01$.

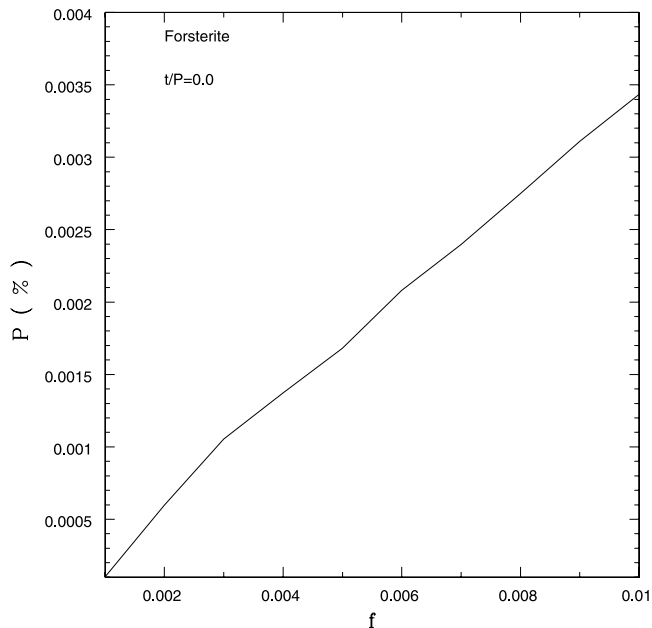


FIG. 3.—Degree of polarization at Bessel *R* band as a function of oblateness f , for a circular orbit with inclination angle $i = 90^\circ$. The linear polarization by a planet with forsterite with $r_0 = 10 \mu\text{m}$ is calculated at the fractional orbital period $t/P = 0.0$.

Consequently, the illuminated area toward the observer increases, yielding a higher amount of polarization that can be seen by the observer.

However, the polarization profile alters drastically when the orbit is noncircular, as can be seen in Figure 4. The degree of polarization peaks when the planet passes its periastron. Hence, the degree of polarization is time variable even if the inclination angle is 0° . The change in the amount of polarization is determined by the eccentricity of the orbit, as can be seen from Figure 5.

As discussed by Brown et al. (1982), the “weighted” or effective optical depth (as seen by the source) of the scattering

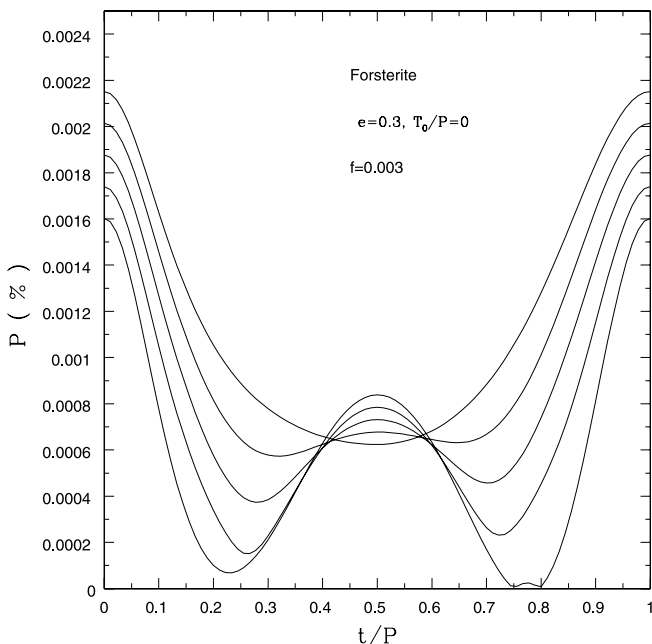


FIG. 4.—Same as Fig. 1, but for planets orbiting in elliptical orbits with eccentricity $e = 0.3$ and epoch of periastron passage $T_0/P = 0$.

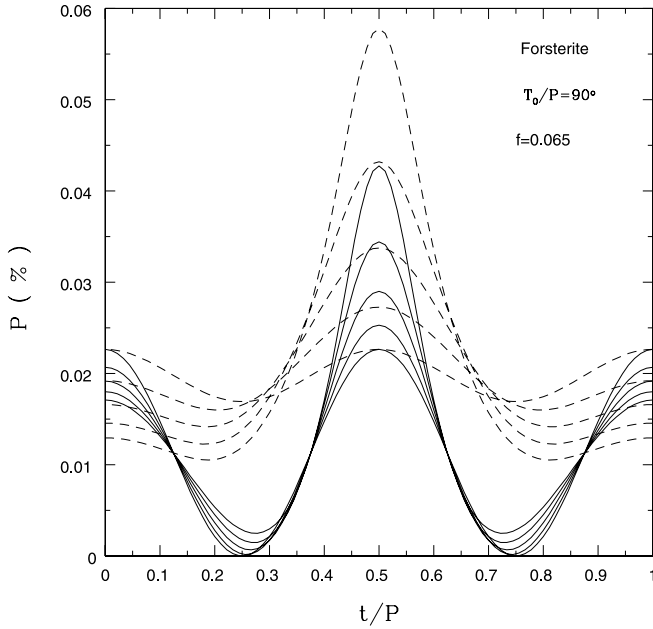


FIG. 5.—Degree of polarization by a planet with $f = 0.065$ and $T_0/P = 0.5$ but different orbital eccentricity, where t/P is the fractional orbital period, t being time and P the orbital period. Solid lines, from bottom to top (at $t/P = 0.5$), represent models with $e = 0.0, 0.1, 0.2, 0.3,$ and 0.4 , respectively, and with $i = 90^\circ$, while the dashed lines represent models with $i = 30^\circ$.

region, idealized as a point scatterer containing N particles, is proportional to the square of the ratio between the semimajor axis a and the stellar separation at longitude λ given by $R(\lambda) = a(1 - e^2)/[1 + e \cos(\lambda - \lambda_p)]$. For a circular orbit this ratio is identically 1, but for an elliptical orbit the ratio is $[1 + e \cos(\lambda - \lambda_p)]/(1 - e^2)$. This means that for an elliptical orbit the effective optical depth of the scattering region as seen by the source is increased by a factor of $h(\lambda, e)$, as given in § 3. For a circular orbit, $e = 0$, and the effective optical depth and hence the degree of polarization becomes independent of the longitude. When $\lambda = \lambda_p$, i.e., when the planet is at periastron, the effective optical depth as seen by the source is at a maximum, yielding the maximum amount of polarization.

As shown by Sengupta & Krishan (2001), Sengupta (2003), and Sengupta & Kwok (2005), the oblateness of the atmosphere plays a crucial role in determining the degree of polarization. The net degree of polarization is calculated by integrating the polarization at all points over the planetary disk. Since we take the number density of scatterers distributed about some symmetry axis, the positive part of polarization is cancelled out by the negative part. As oblateness increases, the net cancellation decreases, owing to the departure from spherical symmetry. Consequently, the disk-integrated polarization would vanish if the geometry were perfectly spherical, and departure from sphericity would give rise to nonzero polarization. An increase in oblateness means more asymmetry and hence more net nonzero polarization. Figure 1 shows that if the oblateness of the planet is as small as 0.003 (similar to that of Earth), then the degree of polarization is of the order of 10^{-4} for the mean grain size of forsterite, $10.0 \mu\text{m}$. The degree of polarization estimated by Seager et al. (2000) for similar planets is of the order 10^{-6} for grain size $1-10 \mu\text{m}$. This is because multiple scattering reduces the amount of polarization by a few orders of magnitude, as discussed in § 2. However, if the oblateness of the object is increased, the degree of polarization increases substantially, as shown in Figure 2, and could be within the range of current detectability. In Figure 3, we

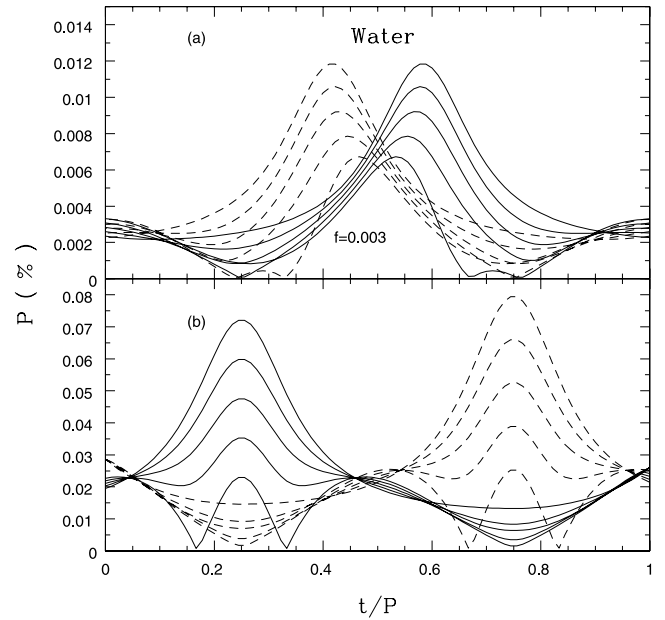


FIG. 6.—Degree of polarization as a function of fractional orbital period t/P at the Bessel R band due to water condensates. (a) Models for a planet with $f = 0.003$, $e = 0.4$, and mean particle radius $r_0 = 5.0 \mu\text{m}$. Solid lines represent models with $\Lambda_p = 60^\circ$ ($T_0/P = 0.58$) and dashed lines represent models with $\Lambda_p = 120^\circ$ ($T_0/P = 0.42$). Both solid and dashed lines, from bottom to top, represent polarization with $i = 90^\circ, 60^\circ, 45^\circ, 30^\circ,$ and 0° , respectively. (b) Same as (a), except that the solid lines represent models with $r_0 = 1.0 \mu\text{m}$, $f = 0.001$, and $T_0/P = 0.25$, while the dashed lines represent models with $r_0 = 4.0 \mu\text{m}$, $f = 0.01$, and $T_0/P = 0.75$.

present the degree of polarization by forsterite grains of mean radius $10 \mu\text{m}$ for different values of planetary oblateness.

Figure 6 shows the polarization profiles of a star with a class II planet that orbits at a distance of $1-2 \text{ AU}$, and hence should have an atmospheric temperature of about 250 K . This type of planet should have a tropospheric cloud layer of water, along with lesser amounts of methane and ammonia.

Although the amount of polarization is dependent on the optical properties of the condensates, the size of the condensates plays a dominant role in determining the amount of polarization. According to the chemical equilibrium model adopted by Cooper et al. (2003), the particle number density increases with decreasing grain size. As a result, the amount of polarization increases substantially when the mean particle size is decreased. Therefore, a high degree of polarization might arise in a less oblate planet if the grain size were sufficiently small. On the other hand, a large amount of polarization can be produced if the grain size is large but the oblateness is high, as shown in Figure 6. In Figure 7, we present the degree of polarization caused by water particulates with different mean sizes. However, in order to understand the effect of grain size, we have kept the T-P profile the same as that calculated by Sudarsky et al. (2003), with mean water particulate size $5 \mu\text{m}$.

It may not be possible to infer from the polarization profile the specific nature of the condensates, the oblateness of the planet, or the orbital inclination angle, as the amount of polarization arises from a combination of all these parameters. However, if the distance of the planet from the primary star is known, the nature of the condensates can be determined. An exact understanding of the chemical equilibrium may provide the size of the condensates. Thus, a combination of the oblateness and the inclination angle of the planet can be determined from the polarization data, which in turn can provide information about the mass and rotational

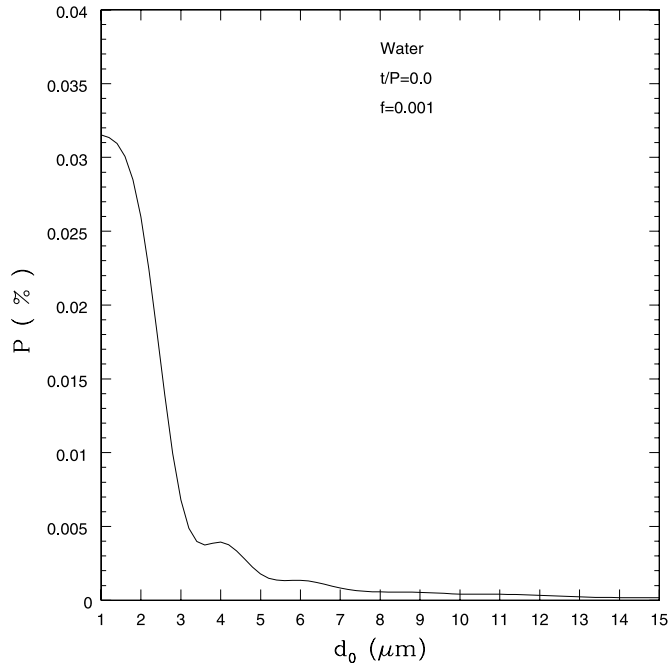


FIG. 7.—Degree of polarization at the Bessel R band as a function of mean grain diameter d_0 . Circular orbit with inclination angle $i = 90^\circ$. The linear polarization by a planet with oblateness $f = 0.001$ having water is calculated at $t/P = 0.0$.

velocity of the planet. However, the periastron angle and orbital eccentricity can be inferred, irrespective of the amount of polarization, from the phase angles at which the maximum and minimum amount of polarization arise.

7. CONCLUSION

The important message that is conveyed in this paper is that single scattering in a rotationally induced oblate planet may

cause an amount of linear polarization sufficient to be detected using available instrumental facilities. The amount of linear polarization would be sufficiently large if the planet is highly oblate and the mean size of the condensates is not greater than a few microns. If detected, the polarization profile will provide information on the oblateness and orbital inclination of the planet and hence on the spin period and mass of the planet. Furthermore, the time-dependent polarization profile would provide the orbital period and eccentricity. Our present discussion is confined to stars with a single planet. The case for more than one planet orbiting a star at different inclinations and phase angles is worth investigating, as that should change the amount and periodic nature of the variability of the polarization. The present investigation is aimed at the polarimetry of known extrasolar planets. Since the orbital separation and the emitted flux from the parent star are known, one can employ theoretical inferences about the composition and location of the condensates in the planetary atmosphere. However, in general, the degree of polarization should depend on the evolution of the planets. Baraffe et al. (2003) have discussed the time evolution of extrasolar planets and showed how the radius and hence the surface gravity, as well as the effective temperature of an irradiated planet, change with time. Since the formation, chemical evolution, and geometrical location of condensates change with the change in surface gravity and atmospheric temperature profile, the degree of polarization, whether by single or multiple scattering, would also alter with time. Therefore, the time evolution of the polarization profile is worth investigating.

We are thankful to the referee for several constructive comments and useful suggestions that have improved the clarity and quality of the paper. This research has made use of NASA's Astrophysics Data System.

REFERENCES

- Ackerman, A. S., & Marley, M. S. 2001, *ApJ*, 556, 872
 Baraffe, I., Chabrier, G., Barman, T. S., Allard, F., & Hauschildt, P. H. 2003, *A&A*, 402, 701
 Barnes, J. W., & Fortney, J. J. 2003, *ApJ*, 588, 545
 Brown, J. C., Aspin, C., Simmons, J. F. L., & McLean, I. S. 1982, *MNRAS*, 198, 787
 Brown, J. C., McLean, I. S., & Emslie, A. G. 1978, *A&A*, 68, 415
 Cooper, C. S., Sudarsky, D., Milsom, J. A., Lunine, J. I., & Burrows, A. 2003, *ApJ*, 586, 1320
 Hubbard, W. B. 1984, *Planetary Interiors* (New York: Van Nostrand Reinhold)
 Mayor, M., & Queloz, D. 1995, *Nature*, 378, 355
 Menard, F., Delfosse, X., & Monin, J. 2002, *A&A*, 396, L35
 Murray, C. D., & Dermott, S. F. 2000, *Solar System Dynamics* (New York: Cambridge Univ. Press)
 Saar, S. H., & Seager, S. 2003, in *ASP Conf. Ser. 294, Scientific Frontiers in Research on Extrasolar Planets*, ed. D. Deming & S. Seager (San Francisco: ASP), 529
 Saumon, D., et al. 2000, *ApJ*, 541, 374
 Scott, A., & Duley, W. W. 1996, *ApJS*, 105, 401
 Seager, S., Whitney, B. A., & Sasselov, D. D. 2000, *ApJ*, 540, 504
 Segelstein, D. J. 1981, M.S. thesis, Univ. Missouri–Kansas City
 Sengupta, S. 2003, *ApJ*, 585, L155
 Sengupta, S., & Krishan, V. 2001, *ApJ*, 561, L123
 Sengupta, S., & Kwok, S. 2005, *ApJ*, 625, 996
 Simmons, J. F. L. 1983, *MNRAS*, 205, 153
 Stam, D. M., Hovenier, J. W., & Waters, L. B. F. M. 2004, *A&A*, 428, 663
 Sudarsky, D., Burrows, A., & Hubeny, I. 2003, *ApJ*, 588, 1121
 van de Hulst, H. C. 1957, *Light Scattering by Small Particles* (New York: Wiley)
 Zapatero Osorio, M. R., Caballero, J. A., & Bejar, V. J. S. 2005, *ApJ*, 621, 445